The proton elastic form factor ratio $\mu_p G_E^p/G_M^p$ at low momentum transfer

G. Ron,[1] J. Glister,[2,3] B. Lee,[4] K. Allada,[5] W. Armstrong,[6] J. Arrington,[7] A. Beck,[8] F. Benmokhtar,[9] B.L. Berman,[10] W. Boeglin,[11] E. Brash,[12] A. Camsonne,[13] J. Calarco,[14] J. P. Chen,[13] Seonho Choi,[4] E. Chudakov,[13] L. Coman,[15] B. Craver,[15] F. Cusanno,[16] J. Dumas,[17] C. Dutta,[5] R. Feuerbach,[13] A. Freyberger,[13] S. Frullani,[16] F. Garibaldi,[16] R. Gilman,[13,17] O. Hansen,[13] D. W. Higinbotham,[13] T. Holmstrom,[18] C.E. Hyde,[19,20] H. Ibrahim,[19] Y. Ilieva,[10] C. W. de Jager,[13] X. Jiang,[17] M. K. Jones,[13] A. Kelleher,[18] E. Khrosinkova,[21] E. Kuchina,[17] G. Kumbartzki,[17] J. J. LeRose,[13] R. Lindgren,[15] P. Markowitz,[11] S. May-Tal Beck,[8] E. McCullough,[2] D. Meekins,[13] M. Meziane,[18] Z.-E. Meziani,[6] R. Michaels,[13] B. Moffit,[18] B.E. Norum,[15] Y. Oh,[4] M. Olson,[22] M. Paolone,[23] K. Paschke,[15] C. F. Perdrisat,[18] E. Piasetzky,[1] M. Potokar,[24] R. Pomatsalyuk,[13,25] I. Pomerantz,[1] A. Puckett,[26] V. Punjabi,[27] X. Qian,[28] Y. Qiang,[26] R. Ransome,[17] M. Reyhan,[17] J. Roche,[29] Y. Rousseau,[17] A. Saha,[13] A.J. Sarty,[2] B. Sawatzky,[15,6] E. Schulte,[17] M. Shabestari,[15] A. Shahinyan,[30] R. Shneor,[1] S. Širca,[24,31] K. Slifer,[15] P. Solvignon,[32] J. Song,[4] R. Sparks,[13] R. Subedi,[21] S. Strauch,[23] G. M. Urciuoli,[16] K. Wang,[15] B. Wojtsekhowski,[13] X. Yan,[4] H. Yao,[6] X. Zhan,[26] and X. Zhu[28]

(The Jefferson Lab Hall A Collaboration)

[1] *Tel Aviv University, Tel Aviv 69978, Israel*
[2] *Saint Mary's University, Halifax, Nova Scotia B3H 3C3, Canada*
[3] *Dalhousie University, Halifax, Nova Scotia B3H 3J5, Canada*
[4] *Seoul National University, Seoul 151-747, Korea*
[5] *University of Kentucky, Lexington, Kentucky 40506, USA*
[6] *Temple University, Philadelphia, Pennsylvania 19122, USA*
[7] *Argonne National Laboratory, Argonne, Illinois 60439, USA*
[8] *NRCN, P.O.Box 9001, Beer-Sheva 84190, Israel*
[9] *University of Maryland, Baltimore, Maryland, USA*
[10] *George Washington University, Washington D.C. 20052, USA*
[11] *Florida International University, Miami, Florida 33199, USA*
[12] *Christopher Newport University, Newport News, Virginia, 2360X, USA*
[13] *Thomas Jefferson National Accelerator Facility, Newport News, Virginia 23606, USA*
[14] *University of New Hampshire, Durham, New Hampshire 03824, USA*
[15] *University of Virginia, Charlottesville, Virginia 22904, USA*
[16] *INFN, Sezione Sanitá and Istituto Superiore di Sanitá, Laboratorio di Fisica, I-00161 Rome, Italy*
[17] *Rutgers, The State University of New Jersey, Piscataway, New Jersey 08855, USA*
[18] *College of William and Mary, Williamsburg, Virginia 23187, USA*
[19] *Old Dominion University, Norfolk, Virginia 23508, USA*
[20] *Université Blaise Pascal / CNRS-IN2P3, F-63177 Aubière, France*
[21] *Kent State University, Kent, Ohio 44242, USA*
[22] *Saint Norbert College, Greenbay, Wisconsin 54115, USA*
[23] *University of South Carolina, Columbia, South Carolina 29208, USA*
[24] *Institute "Jožef Stefan", 1000 Ljubljana, Slovenia*
[25] *Kharkov Institue, Kharkov 310108, Ukraine*
[26] *Massachusetts Institute of Technology, Cambridge, Massachusetts 02139, USA*
[27] *Norfolk State University, Norfolk, Virginia 23504, USA*
[28] *Duke University, Durham, North Carolina 27708, USA*
[29] *Ohio University, Athens, Ohio 45701, USA*
[30] *Yerevan Physics Institute, Yerevan 375036, Armenia*
[31] *Dept. of Physics, University of Ljubljana, 1000 Ljubljana, Slovenia*
[32] *Argonne National Laboratory, Argonne, Illinois, 60439, USA*

(Dated: June 4, 2007)

High precision measurements of the proton elastic form factor ratio, $\mu_p G_E^p/G_M^p$, have been made at four-momentum transfers, Q^2, between 0.2 and 0.5 GeV^2. The new data, while consistent with previous results, clearly show a ratio less than unity and significant differences from the central values of several recent phenomenological fits. By combining the new form-factor ratio data with an existing cross-section measurement, one finds that in this Q^2 range the deviation from unity is primarily due to G_E^p being smaller than the dipole parameterization.

PACS numbers: 13.40.Gp, 25.30.Bf, 24.70.+s, 14.20.Dh

The electromagnetic form factors describe the distribution of charge and magnetism in nuclei. The obser-

vation that the proton form-factor ratio, $\mu_p G_E^p/G_M^p$, is less than unity at $Q^2 > 1$ [1] has led to a renewed experimental focus on the proton electromagnetic form factors [2–11]. Given the long history of form-factor studies, the recent suggestion from a modern form-factor fit that there is structure in each of the four nucleon electromagnetic form factors at $Q^2 < 1$ GeV^2 is intriguing [12] and has been discussed in recent review articles [13–15]. The interest stems from the fact that changes of just a few percent in the nucleon form factors at low Q^2 have direct implications on our understanding of proton structure, as well as on the understanding of many nuclear processes. These include, but are not limited to, parity violation in ep elastic scattering [16–19], deeply virtual Compton scattering [20], and the extraction of the Zemach radius [21].

Figure 1 summarizes the previous data for the proton form-factor ratio for $0.1 < Q^2 < 1$ GeV^2. Many of the recent experiments use polarization techniques [28–30], determining the form-factor ratio using polarized beam and either the ratio of recoil-proton spin components or polarized target asymmetries. The data are from Jefferson Lab Hall A [1, 2, 6, 8, 10], Bates BLAST [11], Mainz A1 [3, 4], and Bates OHIPS [22]. The form factors can also be determined from a Rosenbluth separation of the cross section [31]; the Rosenbluth points in Fig. 1 are taken from the reanalysis by Arrington [23].

The ratio appears to be slightly below unity at lower Q^2, $\sim$0.3 – 0.5 GeV^2. The highest precision extensive data set at low Q^2, from Bates BLAST [11] has two out of the seven points 2σ (statistical) below unity, and the seven points average to 0.990 ± 0.007. If systematic uncertainties are included, no point is significantly lower than 1σ from unity. Figure 1 also shows several recent parameterizations and fits [12, 23–26], along with a light-front cloudy-bag model calculation of the form-factor ratio [27]. The fits and calculation generally show a smooth fall-off of the form-factor ratio with Q^2 that is in overall agreement with the data, but the fits differ from each other and from the data by up to a few percent. While the fits do not include the final BLAST data [11], their variation indicates an improved data base is needed.

In this work we present new measurements of $\mu_p G_E^p/G_M^p$ at Q^2 between 0.2 and 0.5 GeV^2 via the reaction ^{1}H$(\vec{e}, e'\vec{p})$. The experiment was performed in Hall A of the Thomas Jefferson National Accelerator Facility. The longitudinally polarized electrons, $\vec{e}$, were produced from a strained-superlattice GaAs crystal from the photoelectron gun [32] and were accelerated to either 362 or 687 MeV. The beam helicity state was flipped pseudo-randomly at 30 Hz and beam charge asymmetries between the two helicity states were negligible. Due to multi-hall running the degree of longitudinal polarization in Hall A was limited to 40% rather than the full 80%.

The polarized beam was incident on a standard Hall A 4 cm long, liquid hydrogen target [33]. The elastically

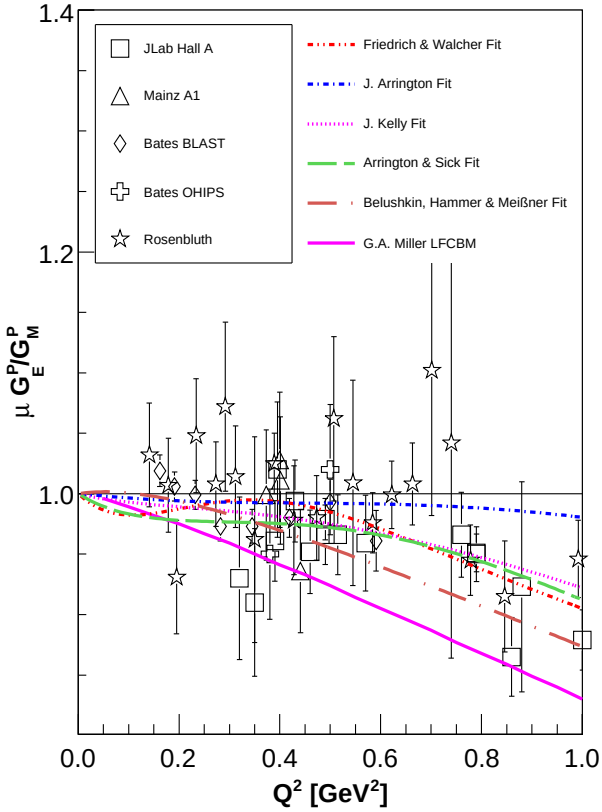

FIG. 1: (Color online) Shown are data for the proton form-factor ratio as a function of four-momentum transfer, Q^2, from previous asymmetry measurements [1–4, 6, 8, 10, 11, 22], as well as from reanalyzed Rosenbluth results [23]. The broken lines are fits [12, 23–26], while the solid line is from a light-front cloudy-bag model calculation [27]. The fits neglect two-photon effect corrections except for that by Arrington & Sick [25] which includes Coulomb corrections. The Arrington fit [23] uses only cross data while the rest include polarization data [12, 24, 26].

scattered protons were detected in the left High Resolution Spectrometer, HRS, which contains a Focal Plane Polarimeter, FPP. When technically possible, the coincident scattered electrons were detected in the right HRS. The scattering angles, momentum, and interaction position at the target of each event were calculated from trajectories measured with vertical drift chambers [34], located in the HRSs. Two planes of plastic scintillators provided triggering and time-of-flight information for particle identification. The FPP, as typically configured [8], consisted of two front and two rear straw chambers, that determine the scattering of particles in a variable thickness carbon analyzer, with density $\approx$1.7 g/cm^3.

The kinematics of the measurements are given in Ta-

ble I. Six of the eight measurements were done as single-arm proton measurements, as obstructions in the Hall prevented detecting electrons at angles larger than 60°. The two lower Q^2 points at 0.687 GeV^2 where measured as *ep* coincidences. The two coincidence points are essentially background free, due to the large *ep* cross section. Coincidence events from the target end-caps, through the Al$(e, e'p)$ reaction, are suppressed by requiring hydrogen elastic kinematics. For the singles data, it is necessary to apply cuts on the target interaction position, and to subtract residual end-cap events using spectra taken on an aluminum dummy target.

TABLE I: Kinematics and FPP parameters for the measured data points. The central spin precession angle is χ. E_e, $\theta_{lab}^{\ p}$ and T_p are the beam energy, proton lab angle and proton kinetic energy, respectively.

Q^2 (GeV^2)	E_e (GeV)	$\theta_{lab}^{\ p}$ (deg)	T_p (GeV)	Analyzer Thickness (inches)	χ (deg)
0.225	0.362	28.3	0.120	0.75	91.0
0.244	0.362	23.9	0.130	0.75	91.9
0.263	0.362	18.8	0.140	0.75	92.7
0.277	0.362	14.1	0.148	0.75	93.4
0.319	0.687	47.0	0.170	2.25	95.3
0.356	0.687	44.2	0.190	3.75	97.0
0.413	0.687	40.0	0.220	3.75	99.6
0.488	0.687	34.4	0.260	3.75	103.0

For scattered protons, the transverse proton polarization components at the focal plane lead to azimuthal asymmetries in re-scattering in the FPP analyzer due to spin-orbit interactions. The alignment of the FPP chambers was determined with straight-through trajectories, with the analyzing material removed. While misalignments and detector inefficiencies lead to false asymmetries, these false asymmetries largely cancel in forming the helicity differences which determine the polarization transfer observables. The transferred polarization was determined by a maximum likelihood method using the difference of the azimuthal distributions corresponding to the two beam helicity states. Previous Hall A measurements of the form-factor ratio used the same procedures [1, 2, 5, 6, 8, 10].

The form-factor ratio is determined from the ratio of polarization transfer components, and thus from the phase shift of the azimuthal scattering distribution in the FPP analyzer. Both the analyzing power and the efficiency cancel out in the calculation of the form-factor ratio; thus, the main issue for systematic uncertainties is spin transport in the spectrometer. The most detailed study of systematics was done for the first Hall A G_E^P experiment [8], which had the FPP mounted in HRS-right. As the spectrometers are nearly identical, it is expected that the limiting systematic uncertainties in this measurement are similar. These uncertainties were about 0.4% at $Q^2 = 0.5$ GeV^2, and rise with Q^2 in the range of that experiment. To control the systematics in this experiment, each polarization point was measured at three different spectrometer central momentum settings, spaced apart by 2 – 3%. In all cases, the polarization values extracted were consistent for the three settings. The uncertainties resulting from the subtraction of residual Al end-cap events were found to be negligible compared with the other systematic uncertainties.

TABLE II: Shown are the experimental ratio results with statistical and systematic errors along with the FPP analyzing power $\langle A_C \rangle$ and efficiency ε_{FPP} for a secondary scattering angle range of 5 to 40 degrees.

Q^2 (GeV^2)	$\langle A_c \rangle$	ε_{FPP} (%)	FOM (%)	$\mu_p G_E^p / G_M^p \pm stat. \pm sys.$
0.225	0.16	1.17	0.03	0.9570 ± 0.0857 ± 0.0036
0.244	0.22	1.03	0.05	0.9549 ± 0.0500 ± 0.0037
0.263	0.24	1.04	0.06	1.0173 ± 0.0495 ± 0.0035
0.277	0.30	1.00	0.09	1.0060 ± 0.0504 ± 0.0030
0.319	0.34	6.05	0.70	0.9691 ± 0.0143 ± 0.0058
0.356	0.36	6.94	0.90	0.9441 ± 0.0099 ± 0.0050
0.413	0.46	4.73	1.00	0.9491 ± 0.0138 ± 0.0053
0.488	0.46	4.73	1.00	0.9861 ± 0.0189 ± 0.0094

The experimental results are summarized in Table II. The average FPP analyzing power $\langle A_c \rangle$ and efficiency ε_{FPP} are consistent with parameterizations of earlier FPP results [35]. The Hall A FPP design allows a much broader angular acceptance than many previous devices, usually limited to about 20°, which leads to a slightly larger efficiency. Also, at the lowest energies, the analyzing power increases at angles beyond 20°, leading to a somewhat larger average analyzing power. The analyzing power quoted is the r.m.s. result, so that the FPP figure of merit, FOM, is given by $\varepsilon_{FPP}\langle A_c \rangle^2$.

The new data, along with other high precision results, are shown in Fig. 2 with the four 362 MeV points of this work having been combined into a single point for plotting. The high statistical precision points at $Q^2 = 0.356$ and 0.413 GeV^2 clearly indicate that $\mu_p G_E^p / G_M^p < 1$. The point at 0.356 (0.413) GeV^2 is 5σ (3.4σ stat. + syst.) below unity; previous data were within $\sim 2\sigma$(stat.) of unity. Compared to the existing fits, the new data in combination with the BLAST data generally indicate that the form-factor ratio lies near the Belushkin *et al.* fit [26] and between the Kelly fit [24] and Miller's calculation [27].

Although a smooth fall-off of $\mu_p G_E^p / G_M^p$ with Q^2 is not ruled out, the new data hint at a possible local minimum in the form-factor ratio at about 0.35 – 0.4 GeV^2. Assuming uncorrelated uncertainties, in the range $Q^2 = 0.3$ – 0.45 GeV^2, we find the world data including the current

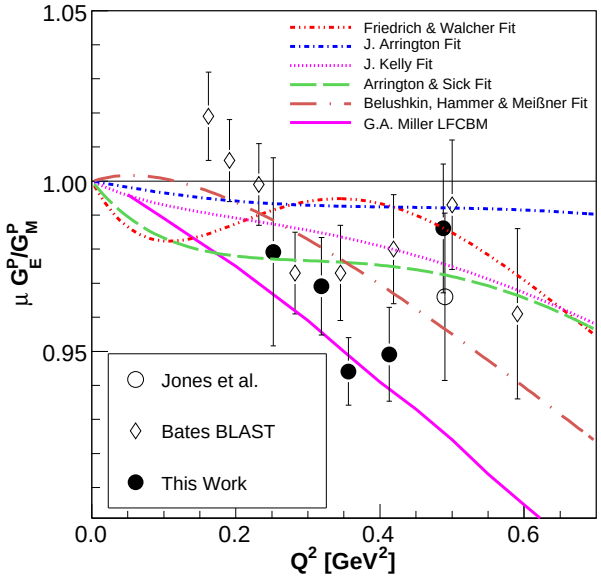

FIG. 2: (Color online) The proton form factor ratio as a function of four-momentum transfer Q^2 shown with world data with total uncertainties below 3% [1, 11]. The broken lines are fits [12, 23–26], while the solid line is from a light-front cloudy-bag model calculation [27].

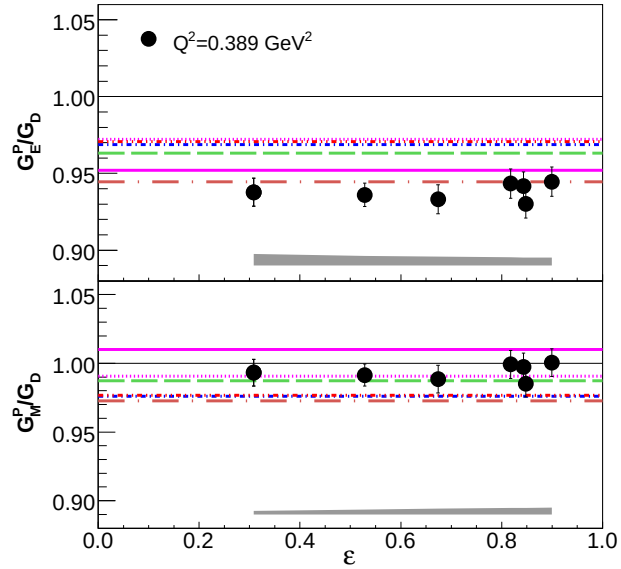

FIG. 3: (Color online) The extracted individual proton form factors as a function of ε. The form factors were obtained for a single Q^2 using the average of the 0.356 and 0.413 GeV^2 data of this work and existing cross-section data at 0.389 GeV^2 [36]. The error bars indicate the statical error of the Berger et al. data while the shaded region indicates how the uncertainty on the asymmetry shifts the points. The systematic uncertainty of the cross section experiment, approximately 2% on each form factor, have not been included.

work average to $0.960 \pm 0.005 \pm 0.005$. This is 3σ lower than the neighboring Q^2 range 0.45 – 0.55 GeV^2, where $\mu_p G_E^p/G_M^p = 0.987 \pm 0.005 \pm 0.006$. In this latter range, the form-factor ratio is only 1.6σ below unity. Theory calculations of the form factors, such as the light-front cloudy bag model calculation by G.A. Miller [27] that is shown, generally show a monotonic decrease of the form-factor ratio.

By combining the present measurement with previous cross-section results, it is possible to extract the individual form factors. Figure 3 shows the individual form factors as a function of ϵ at $Q^2 = 0.389$ GeV^2. These are obtained by combining existing cross-section data with the average of our form-factor ratios from $Q^2 = 0.36$ GeV^2 and 0.41 GeV^2. The figure shows that the form-factor extraction is consistent over the range of ε, the virtual photon polarization. Interestingly, the deviation from unity in the ratio seems to be dominated by the electric form factor. This result is consistent with previous Rosenbluth separation measurements and fits in this region of Q^2; the Rosenbluth results tend to have ∼1–3% uncertainties for each of the form factors, while the fits vary by several percent for each [23].

The comparison of fits with our new results along with the new BLAST results, suggests that a critical reexamination might be needed of experiments (e.g. [18, 20, 37]) that require a knowledge of low Q^2 form factors to a precision of better than ∼3%. For example, for the original HAPPEx result [38] the new data shift the mean about -0.5 ppm, corresponding to a smaller effect from strange quarks, on data with a statistical uncertainty of 1 ppm. More significantly this new result would shift the expected HAPPEx-III result [39] by one standard deviation.

Finally, the low Q^2 proton form-factor database is likely to be improved in the next few years, which should give a clear answer to whether there are few percent structures in the separated form factors or in the ratio $\mu_p G_E^p/G_M^p$. Upcoming results include new cross sections from Mainz [40] and from Hall A [41]. The Hall A cross-section results will be for the same Q^2 as reported herein, and thus will allow a more direct extraction of individual form factors. In addition, the current work is the result of FPP measurements that were run for limited times with limited beam polarization. A dedicated experiment [42] could easily improve the statistical uncertainties by about a factor of three, with normal Jefferson Lab beam polarization and day-long runs, leading to a much improved database for $\mu_p G_E^p/G_M^p$. The results of this work indicate the importance of cross-checking cross-section measurements with high-precision ratio measurements from polarization techniques.

In summary, we have made polarization-transfer measurements to precisely determine the proton form-factor

ratio at low Q^2. We provide definitive evidence that the form-factor ratio differs from unity at low Q^2 and that the deviation is most likely dominated by the electric form factor. Our data suggest a lower value of the ratio and electric form factor than many modern fits. A more definitive measurement is both relatively easy and highly desirable, given the possible implications.

We thank the Jefferson Lab physics and accelerator divisions for their support. This work was supported by the U.S. Department of Energy, the U.S. National Science Foundation, Argonne National Laboratory under contract DE-AC02-06CH11357, the Israel Science Foundation, the Korea Research Foundation, and the US-Israeli Bi-National Scientific Foundation. Jefferson Science Associates operates the Thomas Jefferson National Accelerator Facility under DOE contract DE-AC05-06OR23177. The polarimeter was funded by the U.S. National Science Foundation, grants PHY 9213864 and PHY 9213869.

[1] M. K. Jones et al., Phys. Rev. Lett. **84**, 1398 (2000).
[2] O. Gayou et al., Phys. Rev. C **64**, 038202 (2001).
[3] T. Pospischil et al., Eur. Phys. J. **A12**, 125 (2001).
[4] S. Dieterich, Nucl. Phys. **A690**, 231 (2001).
[5] O. Gayou et al., Phys. Rev. Lett. **88**, 092301 (2002).
[6] S. Strauch et al., Phys. Rev. Lett. **91**, 052301 (2003).
[7] I. A. Qattan et al., Phys. Rev. Lett. **94**, 142301 (2005).
[8] V. Punjabi et al., Phys. Rev. **C71**, 055202 (2005).
[9] M. K. Jones et al., Phys. Rev. **C74**, 035201 (2006).
[10] B. Hu et al., Phys. Rev. **C73**, 064004 (2006).
[11] C. B. Crawford et al., Phys. Rev. Lett. **98**, 052301 (2007).
[12] J. Friedrich and T. Walcher, Eur. Phys. J. **A17**, 607 (2003).
[13] C. E. Hyde-Wright and K. de Jager, Ann. Rev. Nucl. Part. Sci. **54**, 217 (2004).
[14] C. F. Perdrisat, V. Punjabi, and M. Vanderhaeghen (2006), hep-ph/0612014.
[15] J. Arrington, C. D. Roberts, and J. M. Zanotti (2006), nucl-th/0611050.
[16] A. Acha et al., Phys. Rev. Lett. **98**, 032301 (2007).
[17] K. A. Aniol et al., Phys. Rev. Lett. **82**, 1096 (1999).
[18] D. S. Armstrong et al., Phys. Rev. Lett. **95**, 092001 (2005).
[19] F. E. Maas et al., Phys. Rev. Lett. **94**, 152001 (2005).
[20] C. Munoz Camacho et al., Phys. Rev. Lett. **97**, 262002 (2006).
[21] I. Sick, Phys. Lett. **B576**, 62 (2003).
[22] B. D. Milbrath et al., Phys. Rev. Lett. **80**, 452 (1998).
[23] J. Arrington, Phys. Rev. **C69**, 032201(R) (2004).
[24] J. J. Kelly, Phys. Rev. **C70**, 068202 (2004).
[25] J. Arrington and I. Sick (2006), nucl-th/0612079.
[26] M. A. Belushkin, H. W. Hammer, and U.-G. Meissner, Phys. Rev. **C75**, 035202 (2007).
[27] G. A. Miller, Phys. Rev. **C66**, 032201(R) (2002).
[28] A. I. Akhiezer, L. N. Rozentsweig, and S. IM., Sov. Phys. JETP **6** (1958).
[29] N. Dombey, Rev. Mod. Phys. **41**, 236 (1969).
[30] R. G. Arnold, C. E. Carlson, and F. Gross, Phys. Rev. **C23**, 363 (1981).
[31] M. N. Rosenbluth, Phys. Rev. **79**, 615 (1950).
[32] M. L. Stutzman et al., Nucl. Instrum. Meth. **A574**, 213 (2007).
[33] J. Alcorn et al., Nucl. Instrum. Meth. **A522**, 294 (2004).
[34] K. G. Fissum et al., Nucl. Instrum. Meth. **A474**, 108 (2001).
[35] M. W. Mcnaughton et al., Nucl. Instrum. Meth. **A241**, 435 (1985).
[36] C. Berger, V. Burkert, G. Knop, B. Langenbeck, and K. Rith, Phys. Lett. **B35**, 87 (1971).
[37] V. Nazaryan, C. E. Carlson, and K. A. Griffioen, Phys. Rev. Lett. **96**, 163001 (2006).
[38] K. A. Aniol et al., Phys. Rev. **C69**, 065501 (2004).
[39] K. Paschke et al. (2005), Jefferson Lab Experiment E05-109.
[40] J. C. Bernauer et al. (2005), Mainz Experiment **A**1-2/05.
[41] D. W. Higinbotham et al. (2004), Jefferson Lab Experiment E05-004.
[42] G. Ron et al. (2007), Jefferson Lab Proposal PR07-004.

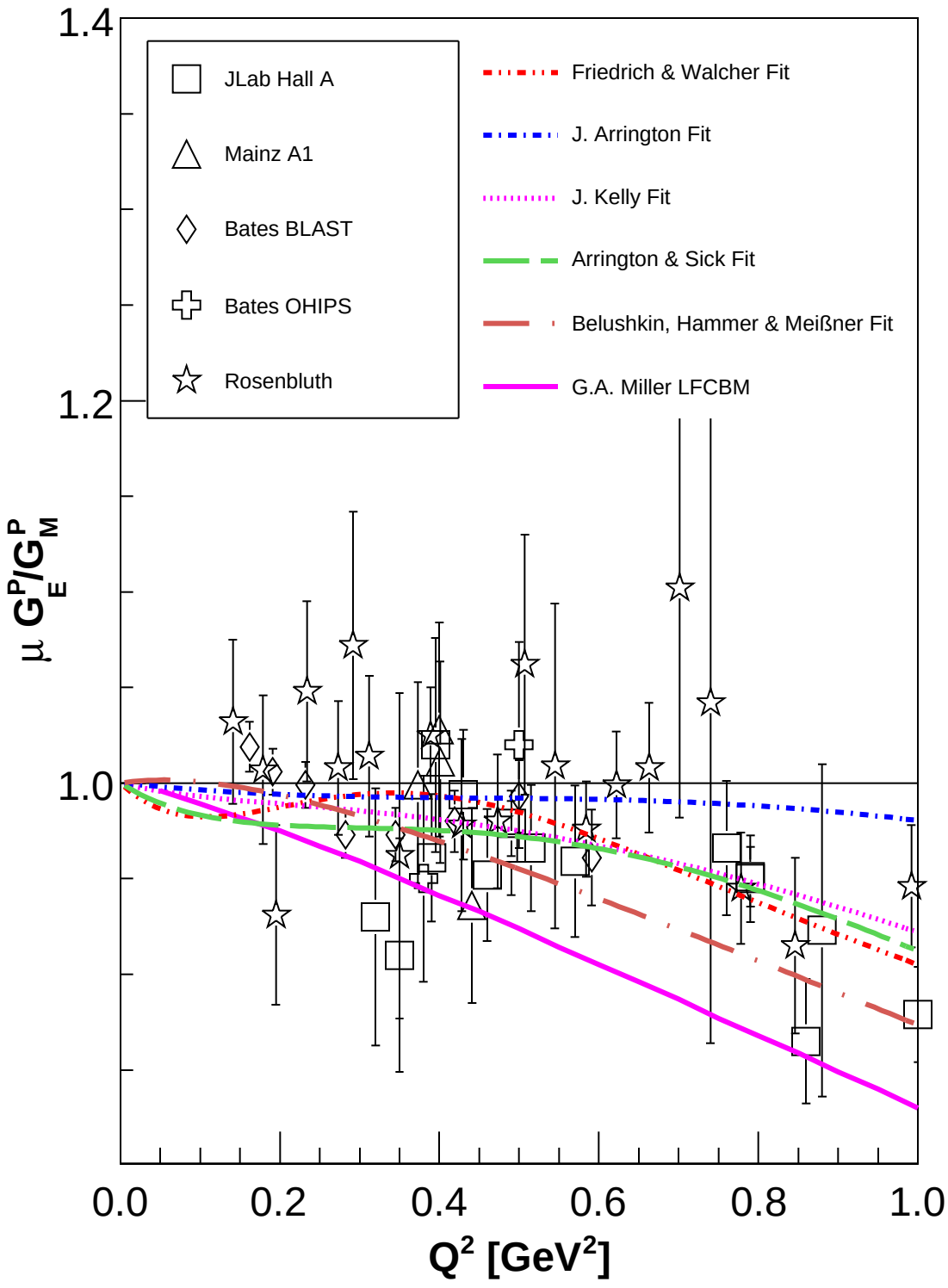
JLab Hall A
Mainz A1
Bates BLAST
Bates OHIPS
Rosenbluth
Friedrich & Walcher Fit
J. Arrington Fit
J. Kelly Fit
Arrington & Sick Fit
Belushkin, Hammer & Meißner Fit
G.A. Miller LFCBM
1.4
1.2
1.0
0.0
0.2
0.4
0.6
0.8
1.0
μ G_E^P/G_M^P
Q² [GeV²]

Figure 1

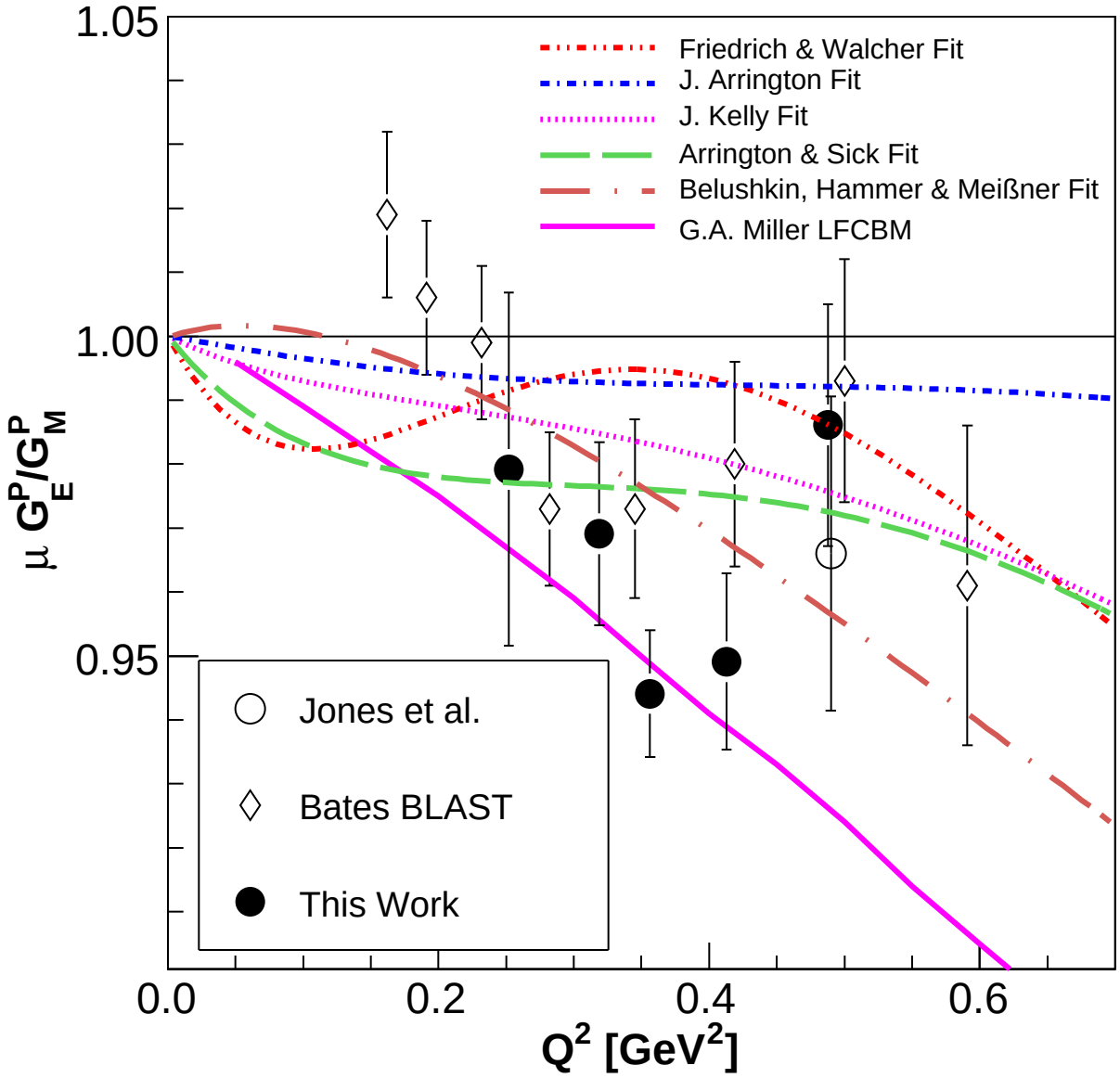
1.05
1.00
0.95
0.0
0.2
0.4
0.6
$\mu G_E^P/G_M^P$
Q^2 [GeV^2]
Friedrich & Walcher Fit
J. Arrington Fit
J. Kelly Fit
Arrington & Sick Fit
Belushkin, Hammer & Meißner Fit
G.A. Miller LFCBM
Jones et al.
Bates BLAST
This Work

Figure 2

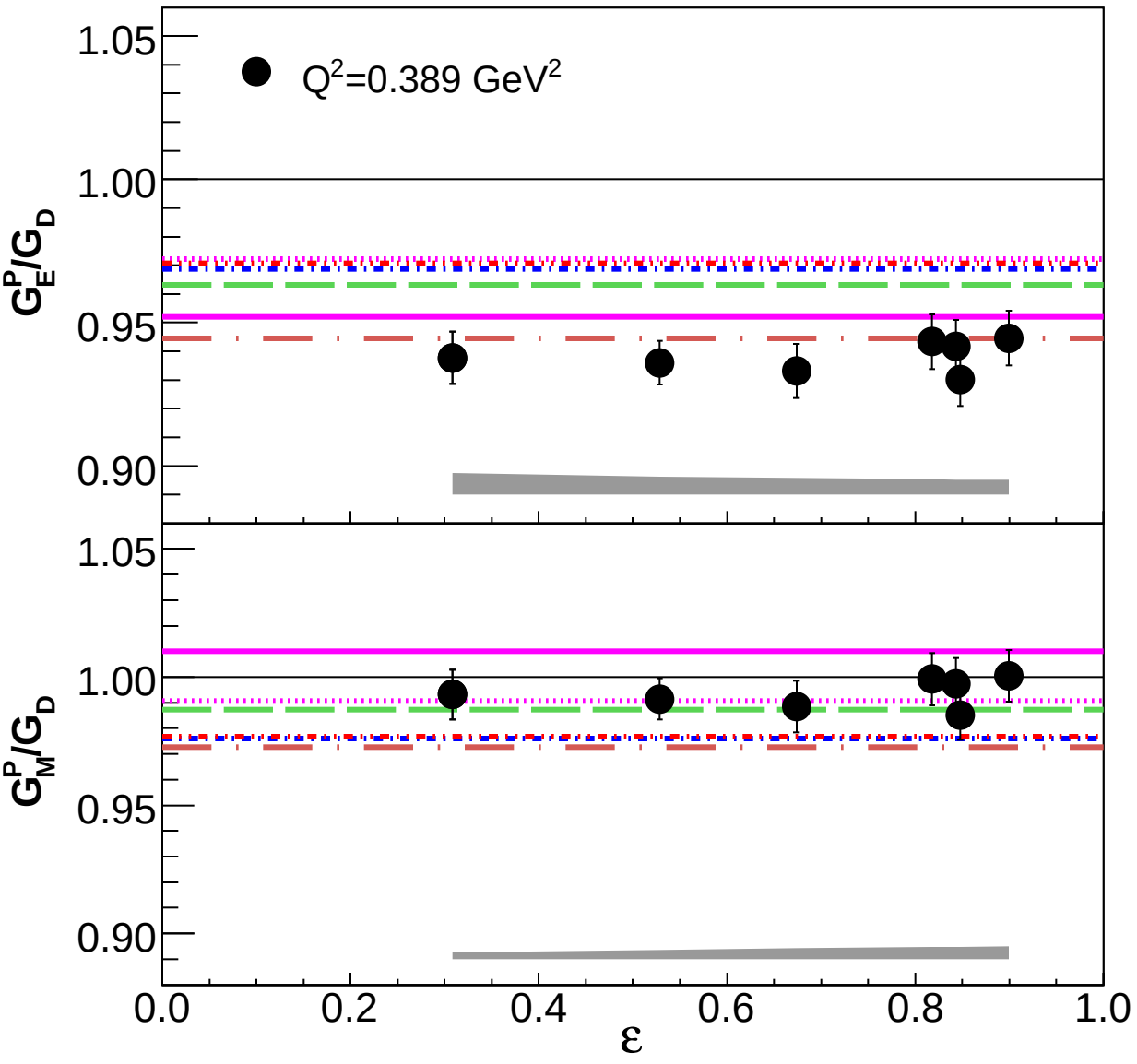
Q²=0.389 GeV²
1.05
1.00
0.95
0.90
G_E^P/G_D
1.05
1.00
0.95
0.90
G_M^P/G_D
0.0
0.2
0.4
0.6
0.8
1.0
ε

Figure 3